

Superconducting quantum metamaterials as an active lasing medium: Effects of disorder

Martin Koppenhöfer,¹ Michael Marthaler,¹ and Gerd Schön^{1,2}

¹*Institut für Theoretische Festkörperphysik, Karlsruhe Institute of Technology, D-76131 Karlsruhe, Germany*

²*Institute of Nanotechnology, Karlsruhe Institute of Technology, D-76344 Eggenstein-Leopoldshafen, Germany*

(Received 9 February 2016; published 8 June 2016)

A metamaterial formed by superconducting circuits or quantum dots can serve as an active lasing medium when coupled to a microwave resonator. For these artificial atoms, in contrast to real atoms, variations in their parameters cannot be avoided. In this paper, we examine the influence of disorder on such a multiatom lasing setup. We find that the lasing process evolves into a self-organized stationary state that is quite robust against disorder. The reason is that photons created by those atoms which are in or close to resonance with the resonator stimulate the emission also of more detuned atoms. Not only the number of photons grows with the number of atoms but also the width of the resonance as a function of the detuning. Similar properties are found for other types of disorder such as variations in the individual coupling. We present relations on how the allowed disorder scales with the number of atoms and confirm it by a numerical analysis. We also provide estimates for the sample-to-sample variations to be expected for setups with moderate numbers of atoms.

DOI: [10.1103/PhysRevA.93.063808](https://doi.org/10.1103/PhysRevA.93.063808)

I. INTRODUCTION

Lasers are the standard sources of coherent light with a wide range of applications [1]. Their basic components are a resonator that stores photons and selects particular modes, an optically active medium that emits photons coherently into the resonator by stimulated emission, and a pumping process that establishes a population inversion in the medium [2]. A large variety of systems can serve as an optically active medium. This includes natural atoms or semiconductor devices [3], but further systems have been proposed and studied experimentally. These include strongly coupled single or few Josephson qubits [4–7] and semiconductor quantum dot systems [8–10]. In these setups, the low number of atoms is compensated by strong coupling. Their frequencies are in the GHz regime; accordingly they are sometimes called “maser” instead of laser. These systems may find useful applications, e.g., as miniaturized on-chip sources of coherent microwaves in low-temperature experiments. There are other on-chip microwave sources which have been studied, including voltage-biased Josephson junctions [11–13] or nonlinear resonators close to the quantum regime [14–16]. However, these devices emit incoherent radiation unless driven by a coherent microwave source. Lasing devices based on qubits also show unconventional properties, such as dressed-state lasing [17,18] or photon-number squeezed light [19,20].

So far, experimental realizations of lasers based on superconducting or quantum dot qubits have only used single or few artificial atoms. A way to reach higher output power is to increase the number M of atoms, e.g., by using superconducting quantum metamaterials. Such materials with 10–100 qubits have already been produced and studied [21]. A drawback of using solid-state circuits is the fact that they invariably suffer from disorder, due to the variations either in the fabrication process or in the environment. As a result, the level-splitting ϵ_j ($j = 1, \dots, M$) and hence the detuning from the resonator frequency $\Delta_j = \epsilon_j/\hbar - \omega$, as well as other parameters such as the coupling strength to the resonator or the local driving, vary for different artificial atoms. We therefore examine the influence of this (quasistatic) disorder on the multiatom lasing.

Our analysis reveals that the lasing process is rather robust against various types of disorder over a wide range of their strengths. The origin of this effect is the following: Those atoms which are above the lasing threshold, e.g., close enough to resonance, start emitting photons into the resonator. These photons enhance the process of stimulated emission, which is proportional to their number $\langle n \rangle$, also for atoms which are still below the threshold. Hence these atoms start participating in the lasing process, and $\langle n \rangle$ grows further. In parallel to this growth, also the range of parameters such as the detuning or coupling strength which are sufficient for lasing increases.

In this paper, we study the effects of disorder in the detuning, the coupling strength, and the pumping strength of the individual atoms on the photon number and the lasing thresholds. After presenting the model and the basic relations in Sec. II, we first compare the single- and the multiatom setups of an ordered system in Sec. III. At this stage we observe already the increase of the allowed range of detuning and the reduced requirement on the coupling strength. In Sec. IV quantitative results are presented for a Gaussian and a box distribution of the disorder in the various parameters. Since probably most experiments in the near future will be carried out with not too large numbers of atoms ($M \lesssim 100$) one should expect significant sample-specific deviations from the average behavior. We therefore also study these statistical properties. In Sec. V we reformulate the problem, which provides further insight into the mechanism responsible for the enhanced stability against disorder.

II. THE MODEL

We model the laser by the standard effective Hamiltonian which accounts only for the two levels which are involved in the lasing transition, and their coherent interaction with the radiation field [2]. For an M -atom system it is the Tavis-Cummings Hamiltonian [22]:

$$H = \hbar\omega a^\dagger a + \sum_{j=1}^M \frac{1}{2} \epsilon_j \tau_z^j + \sum_{j=1}^M \hbar g_j (\tau_+^j a + \tau_-^j a^\dagger). \quad (1)$$

Here a and a^\dagger are the photon annihilation and creation operators of the radiation field. The atoms, labeled by $j = 1, \dots, M$, are modeled as two-level systems with level splitting ϵ_j . The Pauli matrices acting on the two states of atom j are denoted by $\tau_{x,y,z}^j$, and g_j is the coupling strength of atom j to the resonator. The matrices τ_\pm are defined by $\tau_\pm = (\tau_x \pm i\tau_y)/2$. Although this model has been developed for conventional atoms, it also holds for suitable artificial ones, such as superconducting flux and charge qubits or qubits formed by semiconductor quantum dots. The restriction to two levels is valid as long as transitions between further states are sufficiently off resonance. This rules out, e.g., transmon qubits, which have a nearly harmonic level structure, as active lasing material. However, the other mentioned qubits with a sufficiently large anharmonicity can satisfy the requirement, as demonstrated by the experiments with a charge-qubit metamaterial presented in Ref. [21].

Also the pumping can be described in an effective way. Rather than explicitly modeling the pumping, e.g., by transitions via higher states, one can use a quantum master equation approach with effective excitation and relaxation rates of the atom j , $\Gamma_{\uparrow,j}$ and $\Gamma_{\downarrow,j}$, respectively [2,7,23–25]. These rates as well as the pure dephasing rate $\Gamma_{\varphi,j}^*$ of atom j and the relaxation rate κ of the resonator appear in the Lindblad terms of the quantum master equation for the density matrix ρ [26]:

$$\frac{d}{dt}\rho = -\frac{i}{\hbar}[H,\rho] + L_R\rho + \sum_{j=1}^M L_{Q,j}\rho, \quad (2)$$

$$L_R\rho = \frac{\kappa}{2}(2a\rho a^\dagger - a^\dagger a\rho - \rho a^\dagger a), \quad (3)$$

$$\begin{aligned} L_{Q,j}\rho = & \frac{\Gamma_{\downarrow,j}}{2}(2\tau_-^j\rho\tau_+^j - \rho\tau_+^j\tau_-^j - \tau_+^j\tau_-^j\rho) \\ & + \frac{\Gamma_{\uparrow,j}}{2}(2\tau_+^j\rho\tau_-^j - \rho\tau_-^j\tau_+^j - \tau_-^j\tau_+^j\rho) \\ & + \frac{\Gamma_{\varphi,j}^*}{2}(\tau_z^j\rho\tau_z^j - \rho). \end{aligned} \quad (4)$$

The combination of the mentioned rates defines the total relaxation rate $\Gamma_{1,j} = \Gamma_{\uparrow,j} + \Gamma_{\downarrow,j}$ and the total dephasing rate $\Gamma_{\varphi,j} = \Gamma_{1,j}/2 + \Gamma_{\varphi,j}^*$. Below, we will further use the abbreviation $\Gamma_{\kappa,j} = \Gamma_{\varphi,j} + \kappa/2$. By adjusting the rates $\Gamma_{\uparrow,j} > \Gamma_{\downarrow,j}$ we account for the pumping of the lasing medium. Its strength is characterized by the value of the atomic polarization in equilibrium in the absence of a resonator:

$$D_0 = (\Gamma_{\uparrow,j} - \Gamma_{\downarrow,j})/\Gamma_{1,j}. \quad (5)$$

In the following we are mostly interested in the expectation value of the photon number $\langle n \rangle$. It can be obtained with sufficient precision in approaches known as semiclassical or semiquantum laser theory [27]. In these approximations certain expectation values are factorized, which amounts to neglecting certain fluctuations. In the semiclassical theory, all correlations between atomic and resonator states are neglected, equivalent to a factorization of the density matrix, $\rho = \rho_{\text{atom}} \otimes \rho_{\text{res}}$ [28]. This description neglects spontaneous emission, but it yields a good estimate of the lasing threshold. In the semiquantum theory only products of diagonal atomic operators with operators of the radiation field are factorized, e.g., $\langle \tau_z^i a^\dagger a \rangle \approx \langle \tau_z^i \rangle \langle a^\dagger a \rangle$. Furthermore, direct interatomic

couplings are neglected, $\langle \tau_+^i \tau_-^j \rangle \approx 0$ for $i \neq j$. This approach accounts for spontaneous emission and reproduces well the results obtained from a numerical solution of the full master equation (2) [29]. The semiquantum theory leads to the following Maxwell-Bloch equations:

$$\frac{d}{dt}\langle a^\dagger a \rangle = \sum_{j=1}^M i g_j (\langle \tau_+^j a \rangle - \langle \tau_-^j a^\dagger \rangle) - \kappa \langle a^\dagger a \rangle, \quad (6)$$

$$\begin{aligned} \frac{d}{dt}\langle \tau_z^j \rangle = & 2i g_j (\langle \tau_-^j a^\dagger \rangle - \langle \tau_+^j a \rangle) \\ & - \Gamma_{1,j} (\langle \tau_z^j \rangle - D_{0,j}), \end{aligned} \quad (7)$$

$$\begin{aligned} \frac{d}{dt}\langle \tau_+^j a \rangle = & -\left(\Gamma_{\varphi,j} + \frac{\kappa}{2} - i\Delta_j\right)\langle \tau_+^j a \rangle \\ & - i\frac{g_j}{2}(1 + (2\langle a^\dagger a \rangle + 1)\langle \tau_z^j \rangle). \end{aligned} \quad (8)$$

In the stationary state, this set of equations can be cast into a fixed-point equation for the quantum-statistical average photon number $\langle n \rangle = \langle a^\dagger a \rangle$:

$$\langle n \rangle = \sum_{j=1}^M \beta_j \frac{D_{0,j}(\langle n \rangle + \frac{1}{2}) + \frac{1}{2}}{\Gamma_{\kappa,j}^2 + \Delta_j^2 + \alpha_j(\langle n \rangle + \frac{1}{2})}. \quad (9)$$

Here we introduced the parameters

$$\alpha_j = 4g_j^2 \frac{\Gamma_{\kappa,j}}{\Gamma_{1,j}} \quad \text{and} \quad \beta_j = 2g_j^2 \frac{\Gamma_{\kappa,j}}{\kappa}. \quad (10)$$

The term $\langle n \rangle$ on the right-hand side of Eq. (9) accounts for the stimulated emission. Equation (9) is the basic relation for the following analysis.

III. PHOTON NUMBER AND ALLOWED DETUNING OF THE ORDERED SYSTEM

It is instructive to first consider the case without disorder. In this case the fixed-point equation has the solution

$$\langle n \rangle_M^0 = X + \sqrt{X^2 + \frac{M\Gamma_1}{4\kappa}(D_0 + 1)}, \quad (11)$$

$$X = -\frac{1}{4} + \frac{M\Gamma_1}{4\kappa}D_0 - \frac{\tilde{n}_0(\Delta)}{2},$$

$$\tilde{n}_0(\Delta) = \frac{\Gamma_1}{4g^2} \frac{\Gamma_\kappa^2 + \Delta^2}{\Gamma_\kappa}, \quad (12)$$

where the superscript zero refers to the absence of disorder. The quantity $\tilde{n}_0(\Delta)$ is the photon saturation number known already from the semiclassical theory of lasing [6,30]. Within this theory the threshold for lasing is

$$\tilde{n}_0(\Delta) < \frac{M\Gamma_1}{2\kappa}D_0. \quad (13)$$

In Fig. 1 we display how the photon number $\langle n \rangle_M^0(g, \Delta)$ depends on the coupling strength g and the detuning Δ for a many-atom setup with $M = 100$ and the single-atom laser with $M = 1$. Figure 1(a) illustrates the dependence on the coupling strength g . While the many-atom system shows a sharp, kinklike transition to the lasing state above g_{min} , the transition is washed out for the single- and few-atom setup.

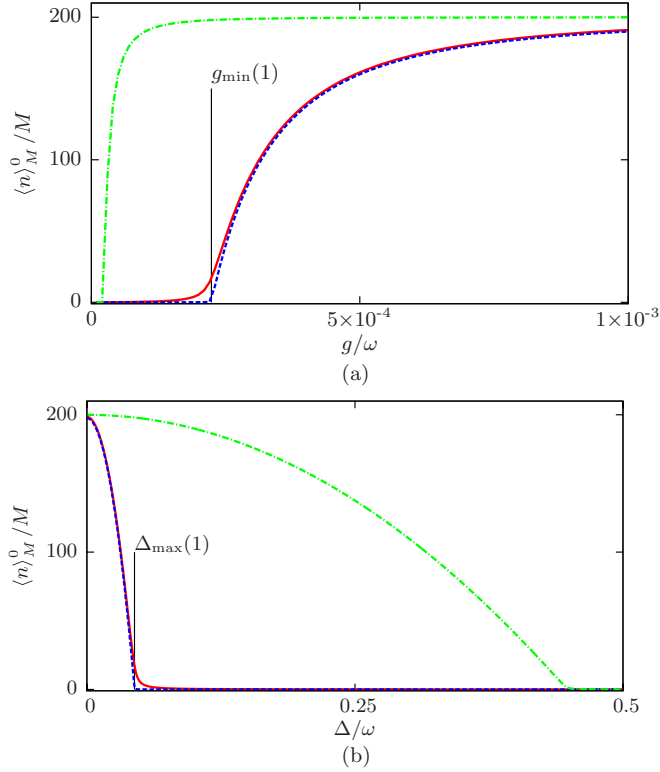


FIG. 1. Properties of the stationary quantum-statistical average photon number $\langle n \rangle_M^0(g, \Delta)/M$ per atom in an ordered lasing setup with M atoms. (a) Plots as a function of the coupling strength g for atoms on resonance, $\Delta = 0 \omega$. (b) Plots as a function of the atomic detuning Δ at $g = 0.002 \omega$. Solid red curves represent $\langle n \rangle_M^0(g, \Delta)$, dashed blue curves represent $\langle n \rangle_M^0(\frac{g}{\sqrt{M}}, \Delta)/M$, and dash-dotted green curves represent $\langle n \rangle_M^0(g, \Delta)/M$. Parameters are $\Gamma_{\uparrow} = 0.006 \omega$, $\Gamma_{\downarrow} = 0.002 \omega$, $\Gamma_{\varphi}^* = 0.001 \omega$, $\kappa = 0.00001 \omega$, and $M = 100$.

However, even for $M = 1$ it remains remarkably sharp. The crossover occurs at

$$g_{\min}(M) = \sqrt{\frac{1}{M} \frac{\kappa}{2D_0} \frac{\Gamma_{\varphi}^2 + \Delta^2}{\Gamma_{\varphi}}} \propto \frac{1}{\sqrt{M}}. \quad (14)$$

As a function of the detuning, illustrated in Fig. 1(b), we note a gradual decrease of $\langle n \rangle_M^0(g, \Delta)$ with increasing Δ , followed by a sharp transition to a low, close to thermal population. The crossover occurs at

$$\Delta_{\max}(M) = \Gamma_{\varphi} \sqrt{2g^2 M \frac{D_0}{\kappa \Gamma_{\varphi}} - 1} \propto \sqrt{M}. \quad (15)$$

The analytic results (14) and (15) follow from Eq. (13), which is, like Eq. (12), obtained within the semiclassical approximation. Strictly, these approximations are valid for very large numbers of M , only. Remarkably they provide good estimates for the thresholds also for small M [5].

The results shown in Fig. 1 also illustrate a remarkable scaling relation [5], namely,

$$\frac{1}{M} \langle n \rangle_M^0 \left(\frac{g}{\sqrt{M}}, \Delta \right) \approx \langle n \rangle_1^0(g, \Delta). \quad (16)$$

The scaling relation, combined with Eqs. (14) and (15), displays the following properties: (i) in the lasing state the number of photons $\langle n \rangle_M^0$ grows linearly with the number of atoms M , (ii) for different M we obtain the same qualitative dependence on the coupling strength provided that it is rescaled as g/\sqrt{M} , and (iii) we furthermore note that the width of the resonance as a function of the detuning increases with the number of atoms proportional to \sqrt{M} . In other words, for a fixed coupling strength, a system with many atoms can tolerate a stronger detuning and still show a transition to the lasing state than a single-atom laser. As we show in Sec. V, this is the reason for the robustness against disorder which we observe in the following section.

In the rest of the paper we focus on disordered systems. Their stationary quantum average photon number is denoted by $\langle n \rangle_M$.

IV. DISORDERED LASING MEDIUM

We now study the lasing transition in a system with many atoms $M \gg 1$ with disorder in either the coupling strength, the detuning, or the pumping. Accordingly, we average Eq. (9) over the appropriate normalized probability distribution:

$$\sum_{i=1}^M \dots = M \iiint d\Delta dg dD_0 p(\Delta, g, D_0) \dots \quad (17)$$

Having carried out the integration, we are left with a fixed-point equation for $\langle n \rangle_M$, depending on M and the distribution p . For clarity we concentrate in the following on disorder in only one lasing parameter at a time.

In general, the problem needs to be solved numerically. However, we can proceed analytically by using a Gaussian distribution p_G or a box distribution p_B :

$$p_G(x) = \frac{1}{\sqrt{2\pi}\sigma_x} \exp\left(-\frac{1}{2} \frac{(x-\mu)^2}{\sigma_x^2}\right), \quad (18)$$

$$p_B(x) = \frac{1}{b} \left[\Theta\left(x - \mu + \frac{b}{2}\right) - \Theta\left(x - \mu - \frac{b}{2}\right) \right], \quad (19)$$

$$b = \sqrt{12} \sigma_x,$$

where x is the variable to be averaged over, μ is its mean value, and σ_x its standard deviation.

Below, we present results for the disorder averages of the quantum-statistical expectation values $\langle n \rangle_M$. On the other hand, an experimental realization of quantum metamaterial-based lasing most likely will not have a very large number M of artificial atoms, and the probability distribution p might not be sampled sufficiently to be well described by the integrals. Instead, for a given realization there will be deviations from the mean value $\langle n \rangle_M$. We analyze these fluctuations numerically by randomly generating setups of M atoms with lasing parameters distributed according to a given probability distribution p , and solving Eq. (9) numerically for each of these setups. The solution for such a random system of M atoms is denoted by $\langle n \rangle_M$. It shows variations from sample to sample.

A. Disorder in the detuning

In this subsection we examine disorder in the atomic detuning $\Delta = \epsilon/\hbar - \omega$. Its average is chosen to be zero. Since the level-splitting energy should be positive, $\epsilon \geq 0$, we have $\Delta \geq -\omega$. This constrains the width of the box distribution to $\sigma_\Delta \leq \omega/\sqrt{3}$. Also in the case of a Gaussian distribution we choose sufficiently narrow distributions to minimize the effect of unphysical values of the detuning. With these restrictions, we average Eq. (9) analytically and obtain

$$\langle n \rangle = M\beta \left[D_0 \left(\langle n \rangle + \frac{1}{2} \right) + \frac{1}{2} \right] I(\zeta_{(n)}), \quad (20)$$

$$\zeta_{(n)} = \sqrt{\Gamma_\kappa^2 + \alpha \left(\langle n \rangle + \frac{1}{2} \right)}.$$

The integrals $I(\zeta)$ for the two types of distributions are given by

$$I_G(\zeta) = \sqrt{\frac{\pi}{2}} \frac{1}{\zeta \sigma_\Delta} \exp\left(\frac{\zeta^2}{2\sigma_\Delta^2}\right) \operatorname{erfc}\left(\frac{\zeta}{\sqrt{2}\sigma_\Delta}\right), \quad (21)$$

$$I_B(\zeta) = \frac{1}{\sqrt{3}\zeta\sigma_\Delta} \arctan\left(\frac{\sqrt{3}\sigma_\Delta}{\zeta}\right). \quad (22)$$

Here, erfc is the complementary error function.

These stationary fixed-point equations can be solved numerically for $\langle n \rangle_M(\sigma_\Delta)$. Results for $M = 100$ atoms are shown by the thick upper curves in Fig. 2 for three values of g and the two types of distribution $p_{G/B}(\Delta)$. We note that disorder in the detuning decreases $\langle n \rangle_{100}(\sigma_\Delta)$ only weakly over a broad range of the standard deviation σ_Δ . This behavior cannot be explained as an average of the single-atom lasing curves $\langle n \rangle_1(\Delta)$, which are displayed in the inset. Averaging them over the distributions $p_{G/B}(\Delta)$ leads to the lower thin dash-dotted and dotted curves in Fig. 2, respectively, which obviously are

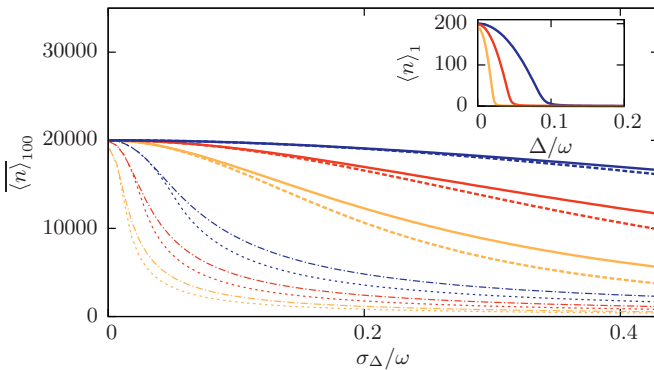


FIG. 2. Influence of disorder in the detuning Δ on the quantum-statistical average photon number $\langle n \rangle_{100}$ in the resonator. Thick solid lines are calculated for a Gaussian distribution with mean $\bar{\Delta} = 0$ and standard deviation σ_Δ ; thick dashed lines represent a box distribution with the same parameters. The average photon number decreases remarkably slowly with increasing disorder. This cannot be explained by averaging the single-atom lasing curves $\langle n \rangle_1(\Delta)$, examples of which are shown in the inset, over the same distribution of detuning. Averaging of the single-atom results would lead to the curves plotted with thin lines. Plot parameters are $M = 100$, $\Gamma_\uparrow = 0.006\omega$, $\Gamma_\downarrow = 0.002\omega$, $\Gamma_\varphi = 0.001\omega$, and $\kappa = 0.00001\omega$; blue (black) curves represent $g = 0.004\omega$, red (gray) curves represent $g = 0.002\omega$, and orange (light gray) curves represent $g = 0.001\omega$.

much narrower in the disorder standard deviation than the collective behavior of the M atoms. We conclude that for disorder in the detuning the setup with M atoms shows lasing in a much broader range of detunings than what we obtain from the single-atom results $\langle n \rangle_1$ averaged over the same probability distribution. We further illustrate this behavior in Sec. V.

In addition we observe that for a weak coupling strength $g = 0.001\omega$ the average contribution of each atom in the M -atom setup in the limit $\sigma_\Delta \rightarrow 0$ is $\langle n \rangle_{100}/100 \approx 200$, whereas $\langle n \rangle_1(\Delta = 0) \approx 195$. That implies that the lasing activity per individual atom is enhanced in the M -atom setup as compared to the single-atom case, although for the parameters considered this is a rather weak effect.

We also note that the results shown for the Gaussian and the box distribution nearly coincide. Both distributions were chosen to have the same average and second-order moment. In addition $\langle n \rangle_M(\sigma_\Delta)$ depends only on even moments of $p_{G/B}(\Delta)$. As a result, for sufficiently narrow distributions, $\sigma_\Delta \ll \omega$, both distributions yield similar results.

We conclude this subsection with an analysis of the sample-to-sample variations of setups with a finite number M of atoms. For this purpose, we consider ensembles with random parameters chosen according to the Gaussian distribution $p_G(\Delta)$ and solve Eq. (9) numerically. Results of $\langle n \rangle_M$, varying around its mean value $\langle n \rangle_M$, are shown in Fig. 3 for the standard deviation $\sigma_\Delta = 0.2\omega$ and $M = 50, 100, 800$, and 1600 atoms. On long enough time scales, when the quasistatic parameters vary in an experiment, we expect that the lasing intensity will vary accordingly.

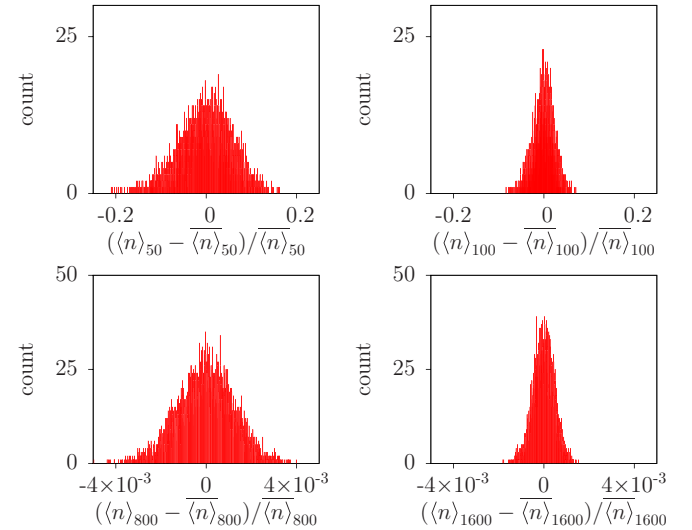


FIG. 3. Fluctuations of $\langle n \rangle_M$ around $\langle n \rangle_M$ for disorder in the detuning due to nonperfect sampling of a Gaussian disorder distribution with $\sigma_\Delta = 0.2\omega$. Histograms are created for 10 000 systems, randomly chosen with the Gaussian distribution, for $M = 50, 100, 800$, and 1600 atoms, respectively. Results are $\langle n \rangle_{50} = 7479$, $\langle n \rangle_{100} = 16976$, $\langle n \rangle_{800} = 156184$, and $\langle n \rangle_{1600} = 316100$ photons with standard deviations of 386, 352, 182, and 136 photons, respectively. Plot parameters are $\bar{\Delta} = 0$, $g = 0.002\omega$, $\Gamma_\uparrow = 0.006\omega$, $\Gamma_\downarrow = 0.002\omega$, $\Gamma_\varphi = 0.001\omega$, and $\kappa = 0.00001\omega$.

B. Disorder in the coupling strength

Similar to the previous case, we examine disorder in the coupling strength g between the atoms and the resonator. The condition $g \geq 0$ imposes rigorous constraints on the box distribution, $\sigma_g \leq \bar{g}/\sqrt{3}$, and similar approximate conditions for the Gaussian distribution.

After averaging, the fixed-point equation (9) becomes

$$\langle n \rangle = \frac{M\Gamma_1}{2\kappa} \left(D_0 + \frac{1}{2\langle n \rangle + 1} \right) I(c_{\langle n \rangle}), \tag{23}$$

$$c_{\langle n \rangle} = \sqrt{\frac{\Gamma_1(\Gamma_k^2 + \Delta^2)}{4(\langle n \rangle + 1/2)\Gamma_k}},$$

with the integrals

$$I_G(c) = 1 - \pi c V(\bar{g}, \sigma_g, c), \tag{24}$$

$$I_B(c) = 1 - \frac{c}{b} \left[\arctan\left(\frac{\bar{g} + b/2}{c}\right) - \arctan\left(\frac{\bar{g} - b/2}{c}\right) \right]. \tag{25}$$

Again, we have $b = \sqrt{12}\sigma_g$, and V is the Voigt function:

$$V(\bar{g}, \sigma_g, x) = \sqrt{\frac{\pi}{2}} \frac{1}{2\pi\sigma_g} \exp\left[-\left(\frac{x - i\bar{g}}{\sqrt{2}\sigma_g}\right)^2\right] \operatorname{erfc}\left(\frac{x - i\bar{g}}{\sqrt{2}\sigma_g}\right) + \text{c.c.} \tag{26}$$

Figure 4 shows numerical solutions $\overline{\langle n \rangle}_M(\sigma_g)$ of these fixed-point equations for $M = 100$ atoms on resonance, $\Delta = 0 \omega$, and for two nonzero values of atomic detuning (thick curves). The mean coupling strength $\bar{g} = 0.001 \omega$ is chosen to be close to the lasing threshold of a single atom on resonance.

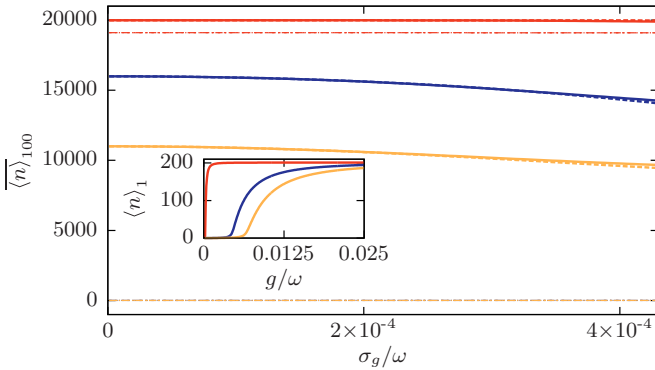


FIG. 4. Influence of disorder in the coupling strength g on the stationary quantum-statistical average photon number $\overline{\langle n \rangle}_{100}$ in the resonator (thick lines). Solid lines are calculated for a Gaussian distribution with mean $\bar{g} = 0.001 \omega$ and standard deviation σ_g ; dotted lines represent a box distribution with the same parameters. The results cannot be explained by averaging the single-atom lasing curves $\langle n \rangle_1(g)$, examples of which are shown in the inset, over the same distribution of the coupling strength. This would yield the results represented by thin lines. Plot parameters are $M = 100$, $\Gamma_{\uparrow} = 0.006 \omega$, $\Gamma_{\downarrow} = 0.002 \omega$, $\Gamma_{\varphi} = 0.001 \omega$, and $\kappa = 0.00001 \omega$. Red (gray) curves represent $\Delta = 0 \omega$, blue (black) curves represent $\Delta = 0.1 \omega$, and orange (light gray) curves represent $\Delta = 0.15 \omega$. The thin blue (black) and orange (light gray) curves coincide.

For disorder in the coupling strength, similar to what we found above, the properties of $\overline{\langle n \rangle}_M$ cannot be explained by averaging the single-atom lasing curves $\langle n \rangle_1(g)$ over the distribution of $p_{G/B}(g)$ (which would result in the thin lines). The averaging yields a smaller average photon number because some of the atoms are coupled with $g < \bar{g}$ and therefore do not contribute (significantly) to the lasing process. On the other hand, the thick red (gray) curve in Fig. 4 shows $\overline{\langle n \rangle}_{100}/100 \approx 200$, hence all atoms are actually participating in the lasing process at their maximum contribution irrespective of their actual individual coupling strength g . This effect is even more pronounced for $\Delta = 0.1 \omega$ or 0.15ω , represented by the thick blue (black) and orange (light gray) curves, respectively, when the single-atom lasing curves and their naïve average predict no lasing activity at all. However, the multiatom setup is still operating at approximately 80 or 50% of its maximum photon number, respectively. In Sec. V we provide further explanations of these properties.

In a typical lasing experiment, the pumping rates are chosen such that the laser operates far above the lasing threshold of a single resonant atom. Then, the decrease in $\overline{\langle n \rangle}_M$ for increasing Δ is even less pronounced than shown in Fig. 4. In this figure we also observe again that the results obtained for a Gaussian and a box distribution coincide for a wide range of the standard deviation σ_g .

We conclude with an analysis of the fluctuations of $\langle n \rangle_M$ around the mean value $\overline{\langle n \rangle}_M$ due to disorder in g for a finite system size M , by the same procedure as described above for the variations in the detuning. The histograms of $\langle n \rangle_M$ in Fig. 5 show a main peak around $\overline{\langle n \rangle}_M$ and a tail representing a few ensembles with much lower $\langle n \rangle_M$. This tail arises because we choose g close to the lasing transition: Some

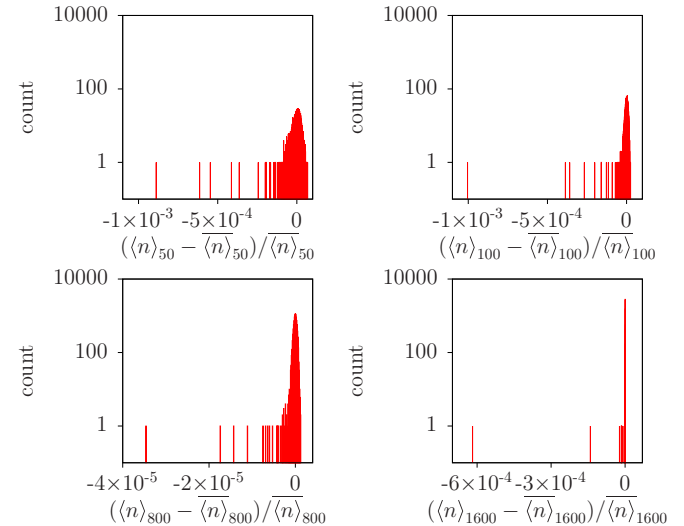


FIG. 5. Fluctuations of $\langle n \rangle_M$ around $\overline{\langle n \rangle}_M$ for disorder in the coupling strength due to a nonperfect sampling of a Gaussian distribution with $\sigma_g = 0.0004 \omega$. Histograms are created for 10 000 systems, randomly chosen with the Gaussian distribution, with $M = 50, 100, 800$, and 1600 atoms, respectively. $\overline{\langle n \rangle}_{50} = 9998$, $\overline{\langle n \rangle}_{100} = 19998$, $\overline{\langle n \rangle}_{800} = 159998$, and $\overline{\langle n \rangle}_{1600} = 319998$. Plot parameters are $\Delta = 0 \omega$, $\bar{g} = 0.002 \omega$, $\Gamma_{\uparrow} = 0.006 \omega$, $\Gamma_{\downarrow} = 0.002 \omega$, $\Gamma_{\varphi} = 0.001 \omega$, and $\kappa = 0.00001 \omega$.

atoms have such weak coupling strengths that they cannot participate in the lasing process. The corresponding systems have effectively a reduced M . As these systems occur rarely, an ensemble of 10 000 systems is not sufficient to produce a smooth distribution. The standard deviation of the main peak is 0.24, 0.17, 0.07, and 0.05 photons, respectively.

C. Disorder in the pumping

The stationary value of the atomic polarization in the absence of a resonator, $D_0 = (\Gamma_\uparrow - \Gamma_\downarrow)/(\Gamma_\uparrow + \Gamma_\downarrow)$, is a function of the pumping and relaxation rates. These rates appear in Eq. (9) via the expressions D_0 and $\Gamma_1 = \Gamma_\uparrow + \Gamma_\downarrow$. In this subsection, we concentrate on the effect of disorder in D_0 while assuming that Γ_1 is fixed. A motivation is provided by the system presented in Ref. [4]. There, the effective excitation and relaxation rates depend on the mixing angle θ of the charge and Josephson energy, which fluctuates because of charge noise. We obtain

$$\Gamma_\uparrow - \Gamma_\downarrow \propto \cos(\theta), \quad (27)$$

$$\Gamma_1 = \Gamma_\uparrow + \Gamma_\downarrow \propto \frac{1}{2}[1 + \cos^2(\theta)]. \quad (28)$$

Typically, we have $\theta \lesssim \pi/2$, so that D_0 fluctuates proportional to $\theta - \pi/2$ whereas Γ_1 is approximately constant.

Averaging Eq. (9) over the disorder in D_0 , we arrive at the fixed-point equation

$$\langle n \rangle = \frac{M\beta[\overline{D_0}(\langle n \rangle + \frac{1}{2}) + \frac{1}{2}]}{\Gamma_\kappa^2 + \Delta^2 + \alpha(\langle n \rangle + \frac{1}{2})}. \quad (29)$$

Its solution is of the same form as Eq. (11), except that D_0 is replaced by $\overline{D_0}$. For resonant atoms above the lasing threshold, Eq. (13) and the relation $\Gamma_1 \overline{D_0} \gg \kappa$ hold. Then, Eq. (11) reduces to a linear dependence on $\overline{D_0}$:

$$\langle n \rangle_M = \frac{M\Gamma_1}{2\kappa} \overline{D_0} - \tilde{n}_0(\Delta). \quad (30)$$

This means that, in contrast to the previously discussed examples, disorder in D_0 is properly accounted for by averaging over the single-atom results $\langle n \rangle_1$.

V. DISCUSSION

The physical origin for the robustness of the system against disorder is an increased stimulated emission of each individual atom if there are additional photons $\langle n_{\text{add}} \rangle$ in the cavity originating from the lasing activity of other atoms. For ordered systems, the enhanced lasing activity, i.e., the growth of the average photon number, $\langle n \rangle_M \propto M$, and the increased range of allowed detuning is explicitly derived from Eq. (9). For disordered systems with disorder in the detuning or the coupling strength, we found a similar behavior of the average quantity $\langle n \rangle_M$. To gain further insight how $\langle n_{\text{add}} \rangle$ additional photons in the resonator broaden and enhance the lasing activity of each individual atom $\langle n_i \rangle$, we split

$$\langle n \rangle = \sum_{j=1}^M \langle n_j \rangle = \langle n_i \rangle + \langle n_{\text{add}}^i \rangle \quad (31)$$

with

$$\langle n_{\text{add}}^i \rangle = \sum_{\substack{j=1 \\ j \neq i}}^M \langle n_j \rangle. \quad (32)$$

Accordingly, we split Eq. (6) into M equations for $\langle n_i \rangle$, which can be interpreted as the contributions of each atom i , and which are given by

$$\langle n_i \rangle = \beta_i \frac{D_{0,i}(\langle n_i \rangle + \langle n_{\text{add}}^i \rangle + 1/2) + 1/2}{\Gamma_{\kappa,i}^2 + \Delta_i^2 + \alpha_i(\langle n_i \rangle + \langle n_{\text{add}}^i \rangle + 1/2)}. \quad (33)$$

If we sum this relation over all $i = 1, \dots, M$, we recover Eq. (9), but it is also valid for the single-atom case, $M = 1$. Since on the right-hand side $\langle n_{\text{add}}^i \rangle$ appears always together with $\langle n_i \rangle$, which is the term describing for a single atom the stimulated emission, the relation displays the property that each individual atom acquires an enhanced lasing activity by the presence of additional photons in the resonator.

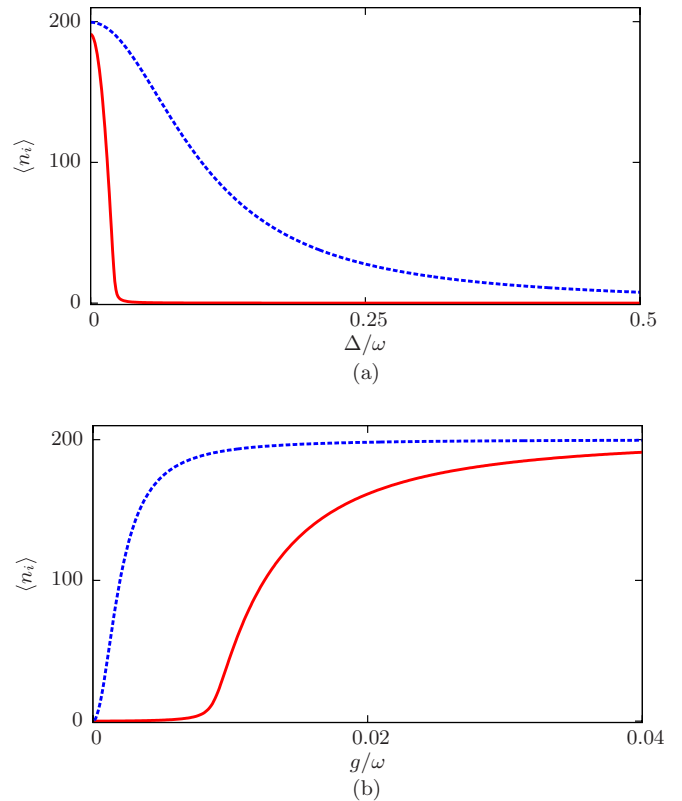


FIG. 6. (a) $\langle n_i \rangle$ as a function of detuning for fixed $g = 0.001 \omega$. (b) $\langle n_i \rangle$ as a function of coupling strength for fixed $\Delta = 0.2 \omega$. Solid red curves represent the case without additional photons in the resonator; dashed blue curves represent the same in the presence of $\langle n_{\text{add}}^i \rangle = 4000$ additional photons in the resonator cavity. Their presence increases the lasing activity of each individual atom as well as the range of allowed detuning, and decreases the threshold coupling strength. Plot parameters are $\Gamma_\uparrow = 0.006 \omega$, $\Gamma_\downarrow = 0.002 \omega$, $\Gamma_\varphi = 0.001 \omega$, and $\kappa = 0.00001 \omega$.

Equation (33) is solved by

$$\langle n_i \rangle = \tilde{X} + \sqrt{\tilde{X}^2 + \frac{\Gamma_{1,i}}{2\kappa} \left[D_{0,i} \left(\langle n_{\text{add}}^i \rangle + \frac{1}{2} \right) + \frac{1}{2} \right]}, \quad (34)$$

$$\tilde{X} = -\frac{1}{4} - \frac{\langle n_{\text{add}}^i \rangle}{2} + \frac{\Gamma_{1,i}}{4\kappa} D_{0,i} - \frac{\tilde{n}_0}{2}.$$

This set of M equations for $\langle n_i \rangle$ has to be solved self-consistently via the relation Eq. (31). This is what we had done (effectively) in the previous parts of the paper both for ordered as well as for disordered systems.

To illustrate the enhancement effect we can also simply assume that there exist additional photons, wherever they come from. Figure 6 compares plots of $\langle n_i \rangle$ for $\langle n_{\text{add}}^i \rangle = 0$ and 4000. Figure 6(a) demonstrates the broadening of the lasing curve as a function of the detuning due to the presence of additional photons, as well as a slight enhancement at $\Delta = 0\omega$, consistent with the observations made in Fig. 2. Figure 6(b) demonstrates the lowering of the lasing threshold coupling strength, consistent with the observations made in Fig. 4.

For disordered setups with a finite-width disorder distribution, we observed that atoms above the lasing threshold, e.g., close enough to resonance, “drag” others, which appeared to be below, also into a lasing state, and finally a self-organized stationary state is established. But we found an enhancement of the lasing window also in the case of ordered systems. Here we like to point out that the reformulation presented in this section can reproduce also this property. To understand it we consider M identical atoms which would all be off-resonant in the single-atom setup, $\Delta > \Delta_{\text{max}}(1)$. It is important to note that the semiquantum model does not exhibit a sharp transition to the lasing state. Therefore, each of the atoms produces a small but nonvanishing contribution $\langle n_i \rangle$ to the total photon number $\langle n \rangle_M^0$. This possibly very small contribution is then enhanced by the presence of all other ones, which may be sufficient to drive the system into the self-consistent broadened state.

VI. CONCLUSION

In this paper, we showed that a multiatom lasing setup with $M \gg 1$ atoms is rather robust against disorder in the individual atomic parameters, e.g., detuning, coupling strength to the resonator, or pumping strength. If an atom is coupled to a cavity that contains additional photons not originating from the atom itself, its lasing activity is nevertheless enhanced because of stimulated emission. This leads to a growth of the number of photons scaling with M , but also to a broadening of the resonance conditions, with the maximum allowed detuning scaling proportional to \sqrt{M} . Therefore, multiple atoms connected to a common resonator can effectively drag each other into resonance and generate a self-consistent stationary state that is robust against disorder.

The average total photon number $\langle n \rangle_M$ of the setup can be calculated by performing the averages implied by the fixed-point equation (9). We have performed these averages for two types of distributions, box and Gaussian, with similar results. Since currently systems with relatively low numbers of artificial atoms ($M \leq 100$) are of interest for lasing experiments, we also examined the fluctuations around $\langle n \rangle_M$ due to the imperfect sampling of the parameter distribution. This provides estimates for sample-to-sample fluctuations in such a lasing setup, as well.

The conclusion from our analysis is that imperfections in the control of material parameters do not prohibit the construction of multiatom lasing setups. This will help the construction of miniaturized on-chip radiation sources for low-temperature microwave experiments.

ACKNOWLEDGMENTS

We acknowledge fruitful discussions with J. Braumüller and H. Rotzinger. This work was supported by the Deutsche Forschungsgemeinschaft Research Grants No. SCHO 287/7-1 and No. MA 6334/3-1.

-
- [1] W. E. Lamb, W. P. Schleich, M. O. Scully, and C. H. Townes, *Rev. Mod. Phys.* **71**, S263 (1999).
 - [2] M. O. Scully and M. S. Zubairy, *Quantum Optics* (Cambridge University, Cambridge, England, 1997).
 - [3] G. H. B. Thompson, *Physics of Semiconductor Laser Devices* (Wiley, New York, 1980).
 - [4] O. Astafiev, K. Inomata, A. O. Niskanen, T. Yamamoto, Yu. A. Pashkin, Y. Nakamura, and J. S. Tsai, *Nature (London)* **449**, 588 (2007).
 - [5] S. André, V. Brosco, A. Shnirman, and G. Schön, *Phys. Rev. A* **79**, 053848 (2009).
 - [6] S. André, P.-Q. Jin, V. Brosco, J. H. Cole, A. Romito, A. Shnirman, and G. Schön, *Phys. Rev. A* **82**, 053802 (2010).
 - [7] D. A. Rodrigues, J. Imbers, and A. D. Armour, *Phys. Rev. Lett.* **98**, 067204 (2007).
 - [8] L. Childress, A. S. Sørensen, and M. D. Lukin, *Phys. Rev. A* **69**, 042302 (2004).
 - [9] P. Q. Jin, M. Marthaler, J. H. Cole, A. Shnirman, and G. Schön, *Phys. Rev. B* **84**, 035322 (2011); J. Jin, M. Marthaler, P. Q. Jin, D. Golubev, and G. Schön, *New J. Phys.* **15**, 025044 (2013).
 - [10] Y.-Y. Liu, J. Stehlik, C. Eichler, M. J. Gullans, J. M. Taylor, and J. R. Petta, *Science* **347**, 285 (2015).
 - [11] M. Hofheinz, F. Portier, Q. Baudouin, P. Joyez, D. Vion, P. Bertet, P. Roche, and D. Esteve, *Phys. Rev. Lett.* **106**, 217005 (2011).
 - [12] V. Gramich, B. Kubala, S. Rohrer, and J. Ankerhold, *Phys. Rev. Lett.* **111**, 247002 (2013).
 - [13] J. Leppäkangas, M. Fogelström, A. Grimm, M. Hofheinz, M. Marthaler, and G. Johansson, *Phys. Rev. Lett.* **115**, 027004 (2015).
 - [14] F. Mallet, F. R. Ong, A. Palacios-Laloy, F. Nguyen, P. Bertet, D. Vion, and D. Esteve, *Nat. Phys.* **5**, 791 (2009).
 - [15] A. Kamal, J. Clarke, and M. H. Devoret, *Nat. Phys.* **7**, 311 (2011).
 - [16] S. Andre, L. Guo, V. Peano, M. Marthaler, and G. Schön, *Phys. Rev. A* **85**, 053825 (2012).

- [17] J. Hauss, A. Fedorov, C. Hutter, A. Shnirman, and G. Schön, *Phys. Rev. Lett.* **100**, 037003 (2008).
- [18] G. Oelsner, P. Macha, O. V. Astafiev, E. Il'ichev, M. Grajcar, U. Hübner, B. I. Ivanov, P. Neilinger, and H.-G. Meyer, *Phys. Rev. Lett.* **110**, 053602 (2013).
- [19] M. Marthaler, J. Leppäkangas, and J. H. Cole, *Phys. Rev. B* **83**, 180505 (2011).
- [20] M. Koppenhöfer and M. Marthaler, *Phys. Rev. A* **93**, 023831 (2016).
- [21] P. Macha, G. Oelsner, J.-M. Reiner, M. Marthaler, S. André, G. Schön, U. Hübner, H.-G. Meyer, E. Il'ichev, and A. V. Ustinov, *Nat. Comm.* **5**, 5146 (2014).
- [22] M. Tavis and F. W. Cummings, *Phys. Rev.* **170**, 379 (1968).
- [23] C. Ginzler, H.-J. Briegel, U. Martini, B.-G. Englert, and A. Schenzle, *Phys. Rev. A* **48**, 732 (1993).
- [24] Y. Mu and C. M. Savage, *Phys. Rev. A* **46**, 5944 (1992).
- [25] S. Ashhab, J. R. Johansson, A. M. Zagoskin, and F. Nori, *New J. Phys.* **11**, 023030 (2009).
- [26] H. Carmichael, *Statistical Methods in Quantum Optics. Vol. 1: Master Equations and Fokker-Planck Equations* (Springer, New York, 1999).
- [27] P. Mandel, *Phys. Rev. A* **21**, 2020 (1980).
- [28] W. Weidlich and F. Haake, *Z. Phys.* **185**, 30 (1965).
- [29] S. André, V. Brosco, M. Marthaler, A. Shnirman, and G. Schön, *Phys. Scr. T* **137**, 014016 (2009).
- [30] The semiclassical approximation is valid in the limit of very large photon numbers, but the parameter $\tilde{n}_0(\Delta)$ appears also in the present semiquantum approximation used to study systems with finite M .